Molecular data, ecological niche, and dispersal models reveal a Trans-Atlantic shallow-water octopus species

Françoise D. Lima[a], Luís Enrique Ángeles-González[b], Hugulay Maia[c], Tatiana S. Leite[d], Miguel Cahuich-López[e,f], Ismael Mariño-Tapia[g], Mariana L. Santana-Cisneros[h], Pedro-Luis Ardisson[h], Sergio M. Q. Lima[a]

[a] Department of Botany and Zoology, Universidade Federal do Rio Grande do Norte, 59078-900, Natal/RN, Brazil

[b] Unidad Multidisciplinaria de Docencia e Investigación-Sisal, Facultad de Ciencias, Universidad Nacional Autónoma de México, Puerto de Abrigo s/n, Sisal, Yucatán, México

[c] Departament of Natural Sciences, Life and Environment, Universidade de São Tomé e Príncipe - USTP, São Tomé, São Tomé and Príncipe

[d] Department of Ecology and Zoology, Universidade Federal de Santa Catarina, 88040-900, Florianópolis/SC, Brazil

[e] Institute of Engineering, National Autonomous University of Mexico, Circuito Escolar, CP 04510, Mexico City, Mexico

[f] NOAA/Air Resources Laboratory, and Earth System Science Interdisciplinary Center/Cooperative Institute for Satellite Earth System Studies, University of Maryland

[g] Escuela Nacional de Estudios Superiores-Mérida,Universidad Nacional Autónoma de México, 97357, Ucú,Yucatán, México

[h] Departamento de Recursos del Mar, Cinvestav. Carretera antigua a Progreso. 97310 Mérida, Yucatán, México

Corresponding author: limad.francoise@gmail.com

ABSTRACT

The tropical *Octopus insularis* is a shallow-water species widely distributed in the western Atlantic. Recent studies of niche models have identified suitable habitats for its settlement

1

27 also on the east coast of the Atlantic. Considering the pelagic larval period and the high

28 tolerance of this species to environmental variations, this study aimed to analyze the

29 possibility of *O. insularis* occurrence in the West Atlantic (São Tomé Island) through

30 molecular analyses, dispersion, and niche models. The molecular analyses were performed

31 using fragments of 481 bp of the mitochondrial gene (cox1) from three muscle samples

32 collected in São Tomé Island. The *O. insularis* long-range connectivity between South

33 America and Western Africa was analyzed using the Lagrangian tool. Additionally, *O.*

34 *insularis* records across its entire known distribution were applied to run the ecological niche

35 model (ENM) using the Maxent algorithm. The Bayesian phylogenetic reconstruction showed

36 that two of the three octopus sequences from São Tomé island (Central-Western Africa)

37 belong to a monophyletic and well-supported *O. insularis* clade. The third octopus sample

38 revealed a new species related to the clade with the *Octopus vulgaris* species complex. The

39 dispersal models pointed out that passive particles could potentially reach the seamounts

40 region at Africa coast via oceanic currents (mainly the North Equatorial Countercurrent) from

41 São Pedro and São Paulo archipelago (Central-Western Region of the Atlantic) in a period

42 of ~30-60 days. This suggests that São Pedro and São Paulo archipelago could act as a

43 potential source of paralarvae to Western Africa, although we hypothesize that this

44 connection was more common during the Pleistocene, when sea level was around 120

45 meters lower. In addition to the already known areas of *O. insularis* occurrence, the ENM

46 pointed suitable habitats to the octopus settlement from Guinea-Bissau down to Equatorial

47 Guinea and Gabon, and African Islands, such as São Tomé and Príncipe. The new record of

48 *O. insularis* in Africa raises important questions regarding regional fisheries management.

49 Considering that *O. insularis* is highly tolerant to environmental variations and very adapted

50 to warm shallow waters, there is a possibility that octopus fisheries stocks on the African

51 coast have a mixed composition (*O. vulgaris*, *O. insularis,* and *Octopus* sp.) and therefore

52 the fisheries must follow management measures suitable for each species. In addition,

53 further studies should be carried out in order to characterize and describe the potential new

54 octopus species found only in São Tomé Island according to our genetic survey.

2

1. Introduction

Dispersal in the marine environment allows individuals (especially in its planktonic stages) to reach long distances and move within and among populations (Cowen and Sponaugle 2009). The ocean circulation, river outflows, thermoclines, and depth can act as "soft" aquatic barriers or even pathways that regulate marine species' movements in the oceanic environment (Hedgecock 1986; Hellberg 2009). Thus, understanding the drivers of larval dispersal in the ocean is a crucial goal for studies on population dynamics, community structure, adaptation, and speciation (Álvarez-Noriega et al. 2020).

Widely distributed species can be interconnected through dispersive processes that promote gene flow among meta-populations. These processes allow populations greater genetic diversity and, consequently, less susceptibility to adverse genetic drift and disappearance by local catastrophes (Hellberg 2009; Nunes et al. 2011). Conversely, isolated populations usually have low genetic diversity, mainly due to genetic drift. However, they may undergo local adaptation processes and give rise to new species along the evolutionary scale, increasing the local diversity of species (Gaither et al. 2015).

Oceanic circulation is one of the main drivers to understanding marine organisms' long-range dispersal. In the tropical Atlantic, surface ocean circulation is delimited by subtropical gyres to the north and south (Lumpkin and Garzoli 2005). The South Equatorial Current (SEC) flows westward and divides into the northern and southern branches at about 12–14°S on the Brazilian coast (Peterson and Stramma 1991). The north branch becomes the North Brazil Current (NBC), which flows bordering the Brazilian coast until the Guyana Current (GC). The south branch of SEC becomes Brazil Current (BC), the western boundary of the South Atlantic subtropical gyre. The retroflection of the NBC flows eastward and forms the North Equatorial

81 Countercurrent (NECC), which extends towards the African coast, turning into the GC

82 (Lumpkin and Garzoli 2005) (Fig. 1).

83 Passive and active trans-Atlantic dispersal processes have been documented for several

84 marine species, including fish, turtles, corals, mollusks, and crustaceans (Joyeux et al. 2001;

85 Lapègue et al. 2002; Rocha et al. 2008; Rudorff et al. 2009; Nunes et al. 2011; Lalire and

86 Gaspar 2019), as well as for some terrestrial groups (Houle 1998; Carranza and Arnold 2003;

87 Renner et al. 2004). Three routes seem to be the main pathway for transoceanic dispersal:

88 from the Caribbean to the Northeast Atlantic, from northern Brazil to the Gulf of Guinea, and

89 from Africa to southern Brazil (Joyeux et al. 2001).

90 Ecological niche modeling performed by Lima et al. (2020) showed suitable areas for *Octopus*

91 *insularis* Leite & Haimocivi, 2008 occurrence along the African coast. However, this species

92 is distributed mainly in the western Atlantic, with the easternmost records in Saint Helena and

93 Ascension islands in the mid-Atlantic (Amor et al. 2017; Lima et al. 2017). Its dispersion ability,

94 generalist diet, and high tolerance level to environmental variation have contributed to its

95 spreading in the West and Mid-Atlantic Ocean waters (Leite et al. 2016; Lima et al.

96 2020). Paralarvae, after hatching, as in many *Octopus* species, spend some time in the water

97 column (1 – 3 months for *O. vulgaris* and *O. americanus*) (Villanueva et al. 1997; Bastos and

98 Vieira 2018; Roura et al. 2019), and are carried by ocean currents across long distances,

99 until settling on the seabed (Boyle and Rodhouse 2005).

100 *Octopus insularis*, most common octopus species in the tropical Atlantic, inhabits shallow

101 waters in a wide range of temperatures and salinities (Leite et al. 2018; Lima et al. 2017). It is

102 found from the subtropical oceanic islands, such as Trindade and Martim Vaz archipelago

103 (20°31'17" S -29°19'18" W), at sea surface temperatures (SST) between 23 and 27 °C (Leite

104 et al. 2009; Leite et al. 2016), to tropical islands such Rocas Atoll (3°51'59" S -33°48'59" W),

105 where the SST reaches up to 36 °C in tide pools inside the atoll ring (Bouth et al. 2011). The

106 embryos of this species also have high thermal tolerance, developing in optimum

107 temperatures around 24-29 °C (Ángeles-González et al. 2020). In addition, *O. insularis* also

4

108 seems to have a high salinity tolerance (Amado et al. 2015), since it has been recorded in

109 estuaries of the Northeastern coast of Brazil and tide pools with high salinities in the Rocas

110 atoll (36 - 42 PSU) (Bouth et al. 2011; Lima et al. 2017).

111 Although *O. insularis* has a wide distribution in the Tropical Atlantic Ocean (Santana-Cisneros

112 et al. 2021; Lima et al. 2022), its long-range transport mechanisms in the Atlantic are still

113 unknown. Previous studies have already pointed out the possibility of *O. insularis* occurrence

114 in the eastern Atlantic (Lima et al. 2020). Therefore, considering the ability of this species to

115 disperse and its wide tolerance for environmental variation, this study aims to use molecular

116 biology methods to confirm the taxonomic status of octopus samples collected on a tropical

117 African island. We also used particle dispersal models to simulate the movement of *O.*

118 *insularis* paralarvae across the tropical Atlantic Ocean and ecological niche models (ENM) to

119 identify regions where it could establish populations in the Americas and Western Africa.

120

121 **2. Material & methods**

122 *2.1 Phylogenetic analyses*

123 *2.1.1 Genetic sample collection*

124 Muscle tissue samples from the arms of three octopus specimens were collected in the Praia

125 Muteca (00° 05' 59.39" N, 06° 37' 34.40" E), Messias Alves (00° 14' 42.56" N, 06° 44' 48.83"

126 E), and Porto Alegre (00° 01' 41.67" N, 06° 30' 44.10" E) from São Tomé Island, about 250

127 km off the African coast, in February 2016. São Tomé Island is characterized by rocky volcanic

128 reefs with limited coral growth. The SST ranges around 26-29°C from September to May and

129 decreases to approximately 25°C from June to August (Maia et al. 2018a). The samples were

130 preserved in 95% ethanol and stored at -10° C. Additional 37 sequences of 14 species were

131 obtained from GenBank to evaluate the phylogenetic relationships among octopod species

132 (Table S1).

133

134 *2.1.2 Molecular analysis*

135 The genomic DNA of octopus specimens was extracted using the GF-1 Nucleic Acid

136 Extraction Kit (Vivantis, Malaysia) following the manufacturer's instructions. Fragments of

137 cytochrome oxidase subunit I gene (*cox*1) were amplified using the universal primers

138 LCO1490 and HCO2198 (Folmer et al. 1994). The PCR amplification reactions were

139 conducted in a final volume of 25 µL containing 1 µL forward primer (10 mM), 1 µL reverse

140 primer, 12.5 µL Taq DNA Polymerase Master Mix (Amplicon A/S, Copenhagen), 8.5 µL H_2O,

141 and 2 µL DNA. PCR cycle parameters used to amplify *cox*1 were 3 min at 95 °C for

142 denaturation, followed by 40 cycles of 1 min at 94 °C, 1 min at 45 °C for annealing, 1.5 min at

143 72 °C for extension, and a final extension step of 4 min at 72 °C. The PCR products were

144 purified and sequenced by Macrogen Inc, Seoul, South Korea.

145 The electropherograms were edited in Geneious 9.0.2 (Kearse et al. 2012), and sequences

146 were aligned using MEGA 6 (Tamura et al. 2013). After sequence alignment, a haplotype

147 distribution was generated using the DNAsp v.5.0 software (Librado and Rozas 2009). The

148 substitution model GTR+G+I was chosen using the software jModeltest (Posada 2008).

149 Bayesian phylogenetic inferences were carried out in BEAST 1.8.4 (Drummond et al. 2012).

150 An uncorrelated lognormal relaxed clock model was used. Monte Carlo Markov Chain

151 (MCMC) runs were performed for 1×10^8 generations, sampling one tree every 1×10^4 runs.

152 The convergence of MCMC runs, effective sample size, and the correct 'burn–in' for the

153 analysis were assessed using Tracer v1.6 (Rambaut et al. 2014). A consensus tree

154 accessing the posterior probability values of each clade was generated using TreeAnnotator

155 1.8.3 (Drummond et al. 2012) and displayed using FigTree 1.4.3. Pairwise genetic distances

156 of an *Octopus* species subset were calculated using Tamura-Nei model distance in MEGA 6

157 (Tamura et al. 2013).

158 *2.2 Ecological Niche Models (ENMs)*

159

6

160 *2.2.1 Occurrence data*

161 *Octopus insularis* records were obtained from the studies of Lima et al. (2020) and Obrien et

162 al. (2021) and combined with supposed occurrences downloaded from the Global Biodiversity

163 Information Facility (GBIF) and Ocean Biodiversity Information System (OBIS) using the

164 libraries rgbif 3.6.0 (Chamberlain et al. 2022) and robis 2.10.1 (Provoost and Bosch 2022)

165 respectively from the software R 4.1.2 (R Core Team 2022). Duplicated, land, or far away

166 records from where *O. insularis* is reported (e.g., depths or latitudes deemed too high) were

167 excluded. In addition, to address the sampling bias of occurrence databases, a random spatial

168 thinning (1000 iterations) with a buffer of 50 km was used with the help of the spThin library

169 (Aiello-Lammens et al. 2015). A total of 54 occurrences remained after the cleaning process.

170 *2.2.2 Environmental layers and calibration region*

171 Maximum, mean, and minimum layers of temperature and salinity were downloaded from Bio-

172 ORACLE (Assis et al. 2017), while bathymetry data and distance to the coast were obtained

173 from MARSPEC (Sbrocco and Barber 2013) at a resolution of ~9 km^2. Five uncorrelated

174 environmental layers (Pearson correlation test, r < |0.8| - Table 1) were kept to avoid model

175 overfitting or wrongly calculated coefficients, as they could hinder the interpretation of our

176 results (Sillero and Barbosa 2021).

177 For model calibration, it is necessary to generate an accessibility hypothesis for model

178 development and testing that represents areas explored by the *O. insularis*. Briefly, the

179 calibration region needs to consider areas within the species' capability of movement, whether

180 it can establish a population or not, allowing us to characterize suitable and unsuitable regions

181 for the species (Barve et al. 2011). Therefore, environmental layers were cropped according

182 to the accessibility hypothesis using the ecoregions by Spalding et al. (2007) (Fig. 1). In

183 addition, variables were masked up to 500 m depth since literature suggests that *O. insularis*

184 benthonic phase is mainly a shallow water species (Batista and Leite 2016; Leite et al. 2009).

7

185 **Table 1.** Environmental variables used to generate a calibration region and develop the

186 ecological niche models (ENM) tested. The asterisk (*) identifies variables used in the ENM

187 after eliminating correlated environmental variables with a Pearson correlation (r > 0.8).

Variable	Key	Measurement unit	Database
Bathymetry*	Bathymetry	m	MARSPEC
Maximum sea surface temperature*	SST_Max	°C	Bio-ORACLE
Mean sea surface temperature	SST_Mean	°C	Bio-ORACLE
Minimum sea surface temperature*	SST_Min	°C	Bio-ORACLE
Range of sea surface temperature	SST_Ran	°C	Bio-ORACLE
Maximum sea surface salinity*	SSS_Max	PSS	Bio-ORACLE
Mean sea surface salinity	SSS_Mean	PSS	Bio-ORACLE
Minimum sea surface salinity*	SSS_Min	PSS	Bio-ORACLE
Range of sea surface salinity*	SSS_Ran	PSS	Bio-ORACLE

188

189 *2.2.3. Model selection and projection*

190 Forty-five Ecological Niche Models (ENMs) of *O. insularis* were generated and selected using

191 the algorithm Maxent v3.4.4 (maxent.jar) via ENMeval library (Kass et al. 2021; Muscarella et

192 al. 2014). Different combinations of features (linear [L], quadratic [Q], product [P], and hinge

193 [H] – L, LQ, LQH, LQP, LQHP) and regularization multipliers (1 to 5 by a sequence of 0.5)

194 were tested for model selection. We used a block partition that divides the data into k-bins

195 (four in this work) based on latitude and longitude (Fig. 1), where occurrences are divided

196 equally as possible (Muscarella et al. 2014), with each bin providing spatially independent

197 evaluation data for models generated by the training data (Radosavljevic and Anderson,

198 2014). This procedure is recommended when extrapolating ENM (Muscarella et al. 2014;

199 Radosavljevic and Anderson 2014).

200 Regarding metrics used for selection, first, we considered models with the lowest omission

201 rate of 10% (OR10); posteriorly, from the remaining models, we selected the ones with the

202 highest AUC validation values (AUCval). Finally, we considered the goodness-of-fit and the

203 complexity, selecting the model with the lowest delta Akaike (delta AIC). The selected model

204 was projected to the East Atlantic region to obtain a suitability map. Later, we created binary

205 maps (presence-absence) based on the minimum presence threshold. This method binarizes

206 the suitability maps based on the lowest value known of an occurrence, allowing us to consider

207 all the information available from known records of *O. insularis*. Since models projections were

208 made in regions away from where the model is calibrated (higher and lower latitudes in the

209 Americas and from Southern Europe to Southern Africa), we used the multivariate

210 environmental similarity surface index (MESS) (Elith et al. 2010) to identify areas of strict

211 extrapolation (i.e., environmental distinct of calibration region) and where caution is needed

212 while interpreting the results.

213

214
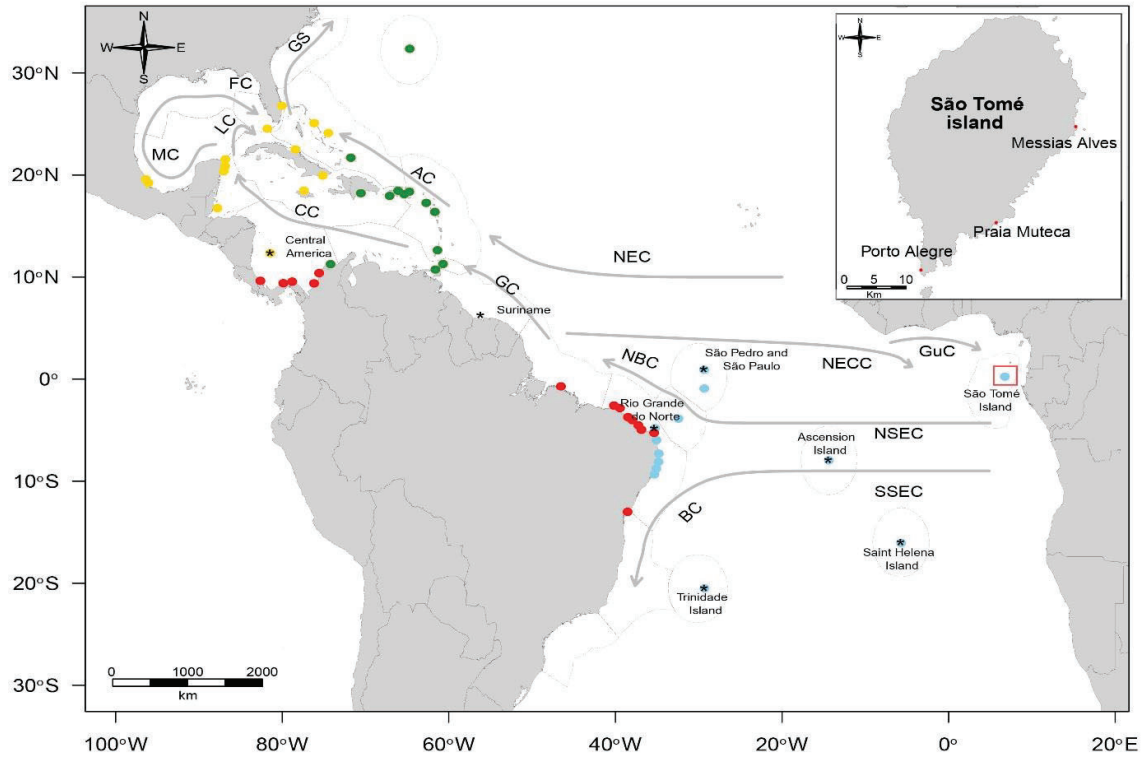
Fig. 1. Occurrences of *Octopus insularis* used for the ecological niche model. Colour dots (yellow, green, red, and blue) indicate the four bins used for model training and testing. Ecoregions by Spalding et al. (2007) used for model calibration are shown as dashed lines. The red square represents São Tome Island (in detail). Ocean currents: northern branch of South Equatorial Current (NSEC), southern branch of South Equatorial Current (SSEC), Brazil Current (BC), North Brazil Current (NBC), Guyana Current (GC), North Equatorial Countercurrent (NECC), Guinea Current (GuC), Caribbean Current (CC), Antilles Current (AC), Loop Current (LC), Mexico Current (MC), Florida Current (FC) and Gulf Stream (GS). Black asterisks indicate release zones used for dispersal models.

2.3 Dispersal model

2.3.1 Dispersal model tool

The *O. insularis* potential long dispersal between South America and Western Africa was analyzed using passive particles from the Lagrangian tool ICHTHYOP v. 3.3.3 (Lett et al.,

10

230 2008) coupled with a hydrodynamic model. ICHTHYOP assesses the effects of physical and

231 biological factors on plankton/particles dynamics and uses as inputs ocean circulation models

232 such as ROMS and MARS (Lett et al. 2008). This software has been extensively used to

233 estimate transport pathways in different organisms (Cabral et al. 2021; Gray et al. 2021;

234 Jordan et al. 2021; Lima et al. 2021; Macías et al. 2021; Santana-Cisneros et al. 2021).

235

236 *2.3.2 Hydrodynamic model*

237 The hydrodynamic model to drive the dispersal model comes from the product GLORYS12V1,

238 a global eddy-resolving physical ocean and sea-ice reanalysis (https://doi.org/10.48670/moi-

239 00021) available in the Copernicus Marine Service (https://www.copernicus.eu/en - CMEMS)

240 with a reliable level of performance reproducing oceanic features such as eddies (Lellouche

241 et al. 2021b, 2021a). This product is based on the current real-time forecasting of the CMEMS

242 system with a model component of NEMO, with the observations assimilated using a reduced-

243 order Kalman filter. The simulation covered the surface waters of the North Atlantic and South

244 Atlantic oceans between 100° W, 20° E and 50° N, 40° S in 1/12° resolution for the period

245 2006-2016 with a daily frequency. The models were reconfigured to a MARS 2D model

246 structure to make them compatible with ICHTHYOP in 2D and tabulated in monthly files.

247

248 *2.3.3 Dispersal model configuration and scenarios*

249 The dispersal implemented a passive Forward Euler time-stepping scheme for advection with

250 a time step of 600 s. With the above configuration, we set seven release zones to seed the

251 initial positions of particles: Rio Grande do Norte, São Pedro and São Paulo archipelago, and

252 Trindade and Martin Vaz, all in Brazil; Suriname; Ascension and Saint Helena islands, and

253 Central America (Fig. 1). The areas were selected aiming to include regions that could help to

254 understand how *O. insularis* disperse in their known distribution (i.e., the whole range of

255 species distribution) and detect potential release regions where sea currents could facilitate a

256 potential connectivity between South America and Africa.

257 In general, there is no evident hatching season for *O. insularis*. Studies on reproduction of this

258 species in the Northeast Brazil found mature males and mature and spawned females

259 occurring year-round (Lima et al. 2014b; Batista et al. 2021). In the Gulf of Mexico, mature

260 and spent females were observed from late spring to autumn, mostly in winter and mature

261 males are present year-round (González-Gómez et al. 2020). Therefore, the models were

262 configured in a forward dispersion approach using a bimonthly simulation starting each month

263 (60 days of time simulation – 12 runs per year, a total of 120 simulations) for the period to

264 establish the potential dates of connectivity between South America and Western Africa. We

265 also accounted for horizontal dispersion in the advection process caused by the turbulent

266 process following Peliz et al. (2007).

267 One hundred thousand particles were released in total for all seven zones, randomly placed

268 in the release zones for each simulation based on *O. insularis* fecundity (68,502 to 120,166

269 oocytes, eggs size ~ 2.5 mm – Lima et al. 2014a, Lenz et al. 2015). It must be pointed out that

270 no study has described the duration of the paralarvae phase of *O. insularis*. However, studies

271 with the related species *O. vulgaris* have demonstrated a planktonic period between 1-3

272 months (Villanueva and Norman 2008). Since *O. insularis* probably has a life cycle shorter

273 than *O. vulgaris* (Lima et al. 2014b, Batista et al. 2021), we decided to settle its planktonic

274 period as 60 days to perform the model simulation.

275

276 **3. Results**

277 *3.1 Genetic analysis*

278 Fragments of 481 bp of the mitochondrial *cox1* gene were used to analyze the phylogenetic

279 relationships among the octopod species. The samples used in the genetic analysis resulted

280 in 30 haplotypes. The Bayesian phylogenetic reconstruction showed that two of the three

281   octopus sequences from São Tomé island belong to a monophyletic and well-supported *O.*

282   *insularis* clade (posterior probability, PP = 1). These specimens are more closely related to

283   the Ascension and Saint Helena individuals, sharing the same haplotype. The *Octopus*

284   *insularis* group splits into two main clades: one with individuals from Trindade and Martin Vaz

285   island and Bahia and the other including octopuses from Northeast Brazil and the Caribbean,

286   where the African samples were placed. The genetic distances between the *O. insularis*

287   individuals from Brazil and Caribbean and the samples from Africa varied between 0.21 to

288   0.84% (Tamura-Nei model) (Table 2), confirming that they belong to the same species.

289   The third octopus sample seems to be a new species related to the clade with the *Octopus*

290   *vulgaris* species complex. Molecular distance analysis showed *O. tetricus* and *O. vulgaris* as

291   the most closely related to this new species, with 91.52% and 91.31% of genetic similarity,

292   respectively (Table 2). A similar analysis performed using BLAST on the NCBI platform

293   revealed a similar result indicating that *O. tetricus* is the most similar species with a 7.55% of
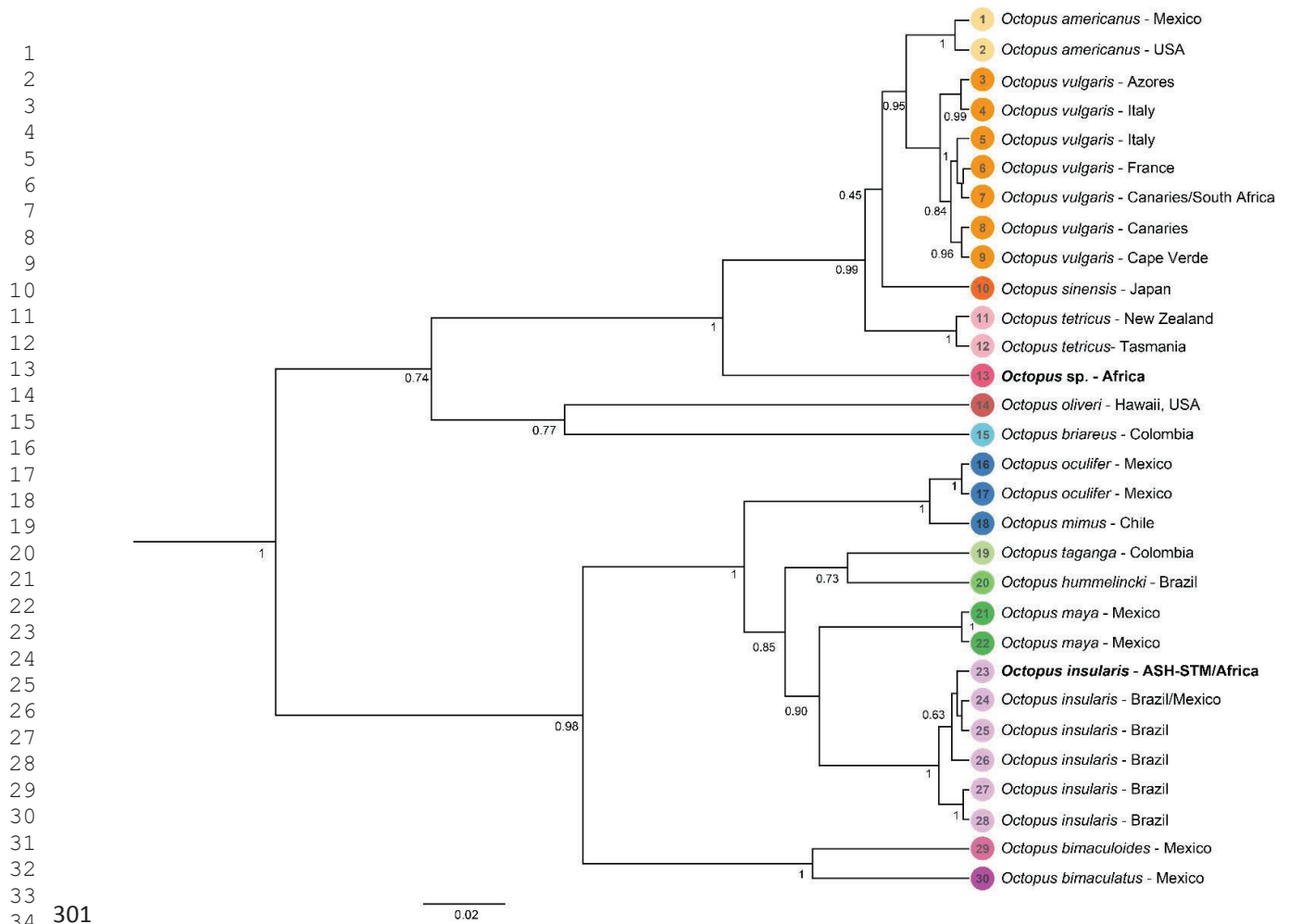
294   genetic distance.

295

296

297

298

299

300

Fig. 2. Bayesian phylogenetic tree constructed with *Octopus cox1* sequences. The Bayesian posterior probabilities of the clades are shown below the nodes. Each color represents a different species. The haplotype number is shown in the circles and detailed in Table S1. In bold are the haplotypes of the African samples collected in this study. ASH = Ascension and St. Helena Islands, STM = São Tomé Island.

14

312 21 **Table 2.** Estimates of evolutionary divergence between sequences of *cox*1 using Tamura-Nei distance. In bold blue are the molecular distances among *O.*

313 23 *insularis* sequences. The genetic distances are estimated in percentage (%). ASH = Ascension and St. Helena Islands, STM = São Tomé Island

Haplotype/Species	1	2	3	4	5	6	7	8	9	10	11	12	13	14	15	16	17	18	19	20	21	22	23	24	25	26	27	28	29
1. *O. americanus* (Mexico)																													
2. *O. americanus* (USA)	0.4																												
3. *O. vulgaris* (Azores)	2.4	2.4																											
4. *O. vulgaris* (Italy)	2.2	2.1	0.2																										
5. *O. vulgaris* (Italy)	2.4	2.4	0.8	0.6																									
6. *O. vulgaris* (France)	2.4	2.4	0.8	0.6	0.4																								
7. *O. vulgaris* (Canaries/South Africa)	2.2	2.1	0.6	0.4	0.2	0.2																							
8. *O. vulgaris* (Canaries)	2.4	2.4	0.8	0.6	0.4	0.4	0.2																						
9. *O. vulgaris* (Cape Verde)	2.8	2.8	1.3	1.1	0.8	0.8	0.6	0.4																					
10. *O. sinensis* (Japan)	3.0	3.0	3.0	2.8	3.0	3.0	2.8	2.6	3.0																				
11. *O. tetricus* (New Zealand)	3.5	3.5	4.2	3.9	4.2	4.2	3.9	3.7	4.2	3.5																			
12. *O. tetricus* (Tasmania)	3.1	3.0	3.7	3.5	3.7	3.7	3.5	3.3	3.7	3.0	0.4																		
13. **Octopus sp.** (STM-Africa)	8.7	8.7	9.2	9.0	9.2	8.7	9.0	8.8	9.3	9.5	9.0	8.5																	
14. *O. oliveri* (Hawaii, USA)	16.3	16.2	16.7	16.5	16.1	16.1	15.8	15.6	16.1	16.3	15.5	15.0	16.1																
15. *O. briareus* (Colombia)	15.8	15.7	17.3	17.6	17.9	17.3	17.6	17.4	17.3	17.1	15.8	15.5	16.7	15.9															
16. *O. oculifer* (Mexico)	13.4	13.3	15.0	14.7	15.0	15.0	14.7	14.5	14.0	14.0	13.9	13.4	13.5	16.4	16.4														
17. *O. oculifer* (Mexico)	13.6	13.6	14.7	14.4	14.7	14.7	14.4	14.2	13.7	13.7	13.6	13.1	13.8	16.8	16.7	0.2													
18. *O. mimus* (Chile)	13.0	13.0	14.6	14.4	14.6	14.7	14.4	14.2	14.1	13.7	13.6	13.0	13.8	15.8	16.0	1.1	1.3												
19. *O. taganga* (Colombia)	14.2	14.1	15.2	15.0	15.8	15.3	15.6	15.3	15.3	14.9	14.1	13.6	14.0	15.1	14.9	4.7	4.9	4.4											
20. *O. hummelincki* (Brazil)	14.3	14.3	14.8	14.5	15.4	15.4	15.1	15.4	15.3	14.6	14.7	14.2	15.2	16.5	16.4	6.6	6.9	6.3	4.9										
21. *O. maya* (Mexico)	16.3	16.2	16.4	16.2	17.1	16.5	16.8	16.6	16.5	16.6	16.8	16.3	15.0	17.9	17.3	8.1	7.8	7.8	7.6	8.7									
22. *O. maya* (Mexico)	16.6	16.5	16.7	16.5	17.4	16.8	17.1	16.9	16.8	16.9	17.2	16.6	15.3	18.3	17.6	8.4	8.1	8.0	7.9	8.9	0.2								
23. **O. insularis** (ASH-STM/Africa)	12.0	11.9	12.4	12.2	13.0	13.0	12.7	12.5	12.5	12.6	13.0	12.5	15.0	16.3	17.4	6.4	6.6	6.1	6.5	7.5	8.8	9.1							
24. *O. insularis* (Brazil)	12.3	12.2	12.7	12.5	13.3	13.3	13.0	12.8	12.7	12.9	13.3	12.8	14.7	16.0	17.7	6.1	6.4	5.8	6.2	7.2	8.6	8.8	**0.2**						
25. *O. insularis* (Brazil)	12.5	12.5	13.0	12.7	13.6	13.6	13.3	13.1	13.0	13.2	13.6	13.1	15.0	16.0	18.0	6.4	6.6	6.1	6.5	7.5	8.3	8.5	**0.4**	**0.2**					

15

26. *O. insularis* (Brazil)	12.5	12.5	13.0	12.7	13.6	13.6	13.3	13.1	13.0	13.2	13.6	13.1	14.4	16.3	18.0	6.4	6.6	6.1	6.5	7.5	8.3	8.5	0.4	0.2	0.4					
27. *O. insularis* (Brazil)	12.8	12.7	13.0	12.7	13.5	13.6	13.3	13.1	13.0	13.2	13.3	12.8	14.7	15.7	18.3	6.3	6.6	6.0	6.4	7.4	8.7	9.0	0.8	0.6	0.8	0.8				
28. *O. insularis* (Brazil)	12.8	12.7	13.0	12.7	13.5	13.6	13.3	13.1	13.0	13.2	13.3	12.8	14.7	15.7	18.3	6.3	6.6	6.0	6.4	7.4	8.9	9.2	1.1	0.8	1.1	1.1	0.2			
29. *O. bimaculoides* (Mexico)	15.7	16.3	17.1	16.9	17.8	17.2	17.5	17.3	17.2	16.5	17.6	17.0	15.9	19.1	15.7	11.5	11.8	11.7	11.1	12.5	12.6	12.9	11.4	11.1	11.4	11.4	11.8	11.8		
30. *O. bimaculatus* (Mexico)	15.2	15.1	15.9	15.7	16.6	16.0	16.3	16.1	16.0	16.6	17.7	17.1	15.6	15.9	16.4	11.6	11.9	10.7	11.1	12.0	12.4	12.7	11.7	11.4	11.7	11.7	11.6	11.6		6.7

3.2 Ecological Niche Model

316 The ENM with the best overall performance had an L configuration (AUCval = 0.78, OR10 =

317 0.05 and delta AIC = 5.69). The permutation importance analysis indicates that the variables

318 that most contributed to the model were SST_Min (44.1%), SSS_Min (27.9%), and Bathymetry

319 (26.6%). Conversely, SST_Max contributed little (1.4%), while SSS_Max and SSS_Ran effect

320 on the model was negligible (0%). Suitability maps were binarized according to a value of 0.19

321 (Fig. S1), meaning that any value below was considered an absence. Response curves (Fig.

322 S2) show that *O. insularis* has high thermal (from 20 °C to temperatures above 30 °C) and

323 salinity tolerances (20 PSS – Fig. S2).

324 Suitability (Fig. 3) and binary map (Fig. S2) suggest that the distribution of *O. insularis* in

325 America occurs from Florida, USA (~30°N) to São Paulo and Paraná, Brazil (~25°S – however,

326 such southern regions have lower suitability) with Amazon River acting as a soft barrier. This

327 species could also find potentially suitable regions throughout the Gulf of Mexico (except the

328 Northern Gulf of Mexico) and the Caribbean. The Mid-Atlantic islands like São Pedro and São

329 Paulo, Ascension, Saint Helena, and Trindade and Martin Vaz may harbor octopus

330 populations. Regarding Western Africa, suitable regions are found from Guinea-Bissau

331 (~12°N) down to Equatorial Guinea and Gabon (~1°N), with a break of suitability in front of

332 coastal Cameroon (~3°N). Finally, the ENM also suggests that the African Islands such as

333 São Tomé and Príncipe, and Cabo Verde have favorable environmental conditions. High

334 extrapolation risk was detected in northern and southern Africa (Fig. S3).

335

336

337

338

339

340

17
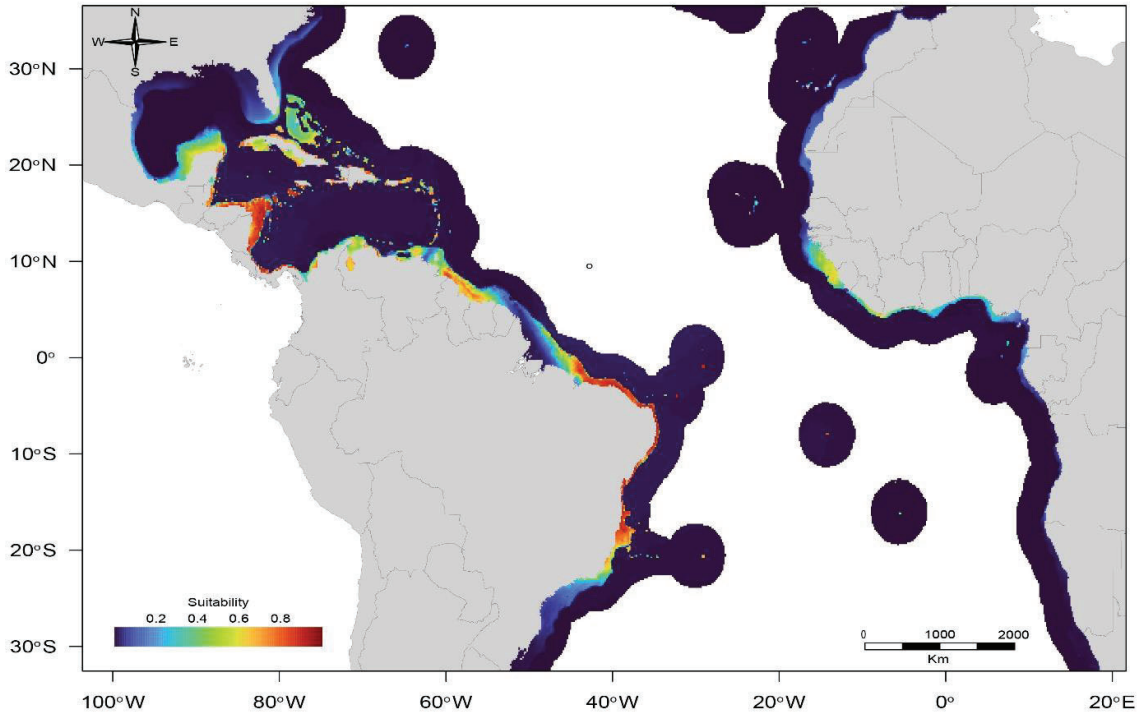
Fig. 3. Distribution of suitable climatic niche for *Octopus insularis* in the Atlantic Ocean

3.3 Dispersal models

3.3.1 Bimonthly dispersal simulations

The bimonthly simulations (simulations of 60 days) showed that particles from northeast coast of Brazil, Suriname, Caribbean regions of Colombia, and Central America tend to disperse toward the northwest Atlantic, the latter arriving in Florida. In addition, the São Pedro and São Paulo archipelago could have acted as a stepping-stone between South America and Western Africa thanks to the Equatorial Countercurrent, allowing particles to get closer to seamounts region at Central-West Africa in 30-60 days approximately. May and June are the months that showed higher potential connectivity between São Pedro and São Paulo and the African coast, mainly in 2009 when particles reach close the African Shelf. Finally, Trindade and Martim Vaz, Ascension, and Saint Helena islands greatly differed from the other release zones since the dispersion was almost non-existent (Fig. 4), with no connectivity between them or other

release regions. The gifs animation files of bimonthly dispersal simulations for the years 2006

357 to 2015 are shown in Supplementary 4.

358

359
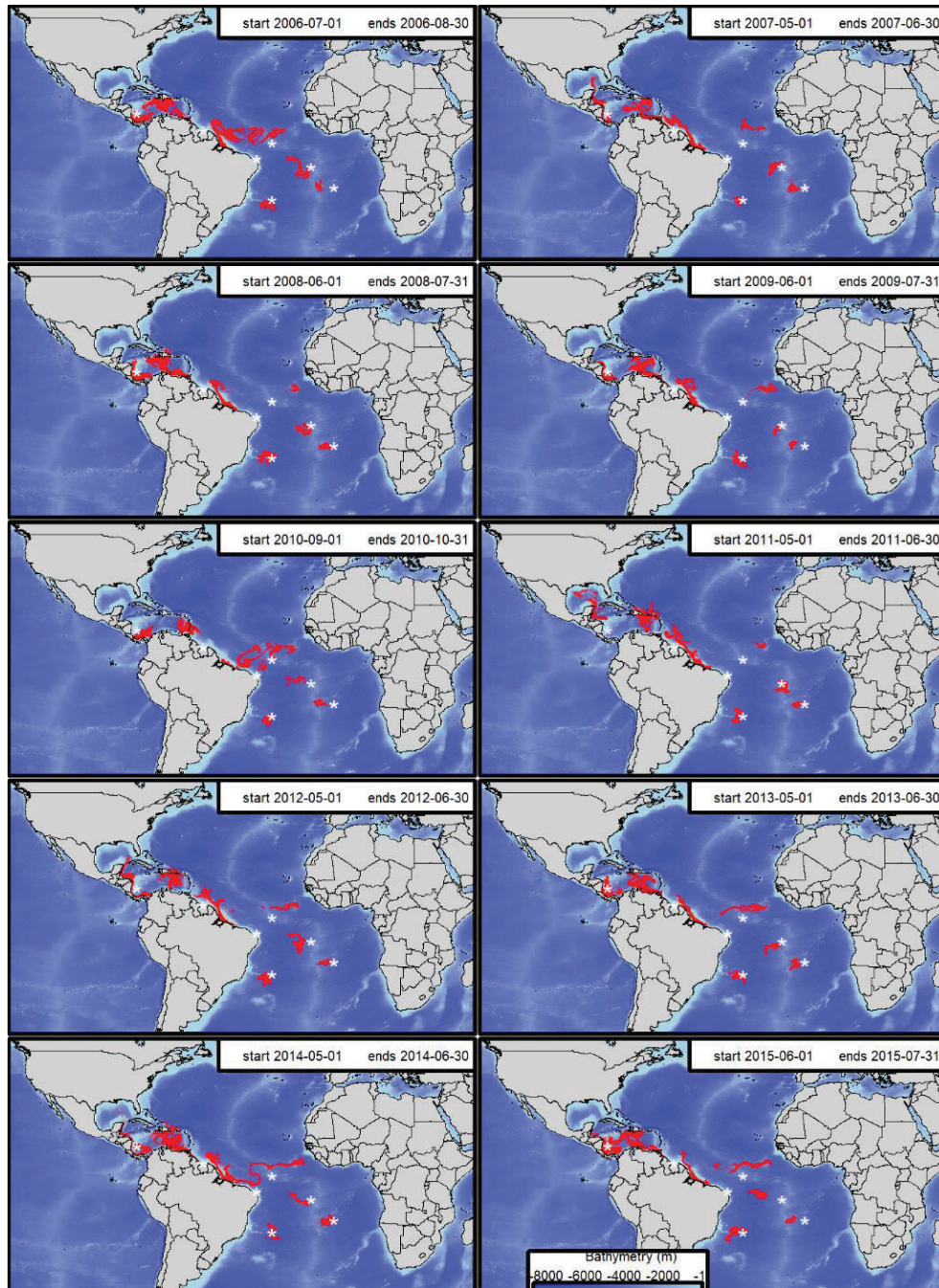
Fig. 4. Bimonthly dispersal simulations of *Octopus insularis* paralarvae. The stars indicated

361 the released areas.

4. Discussion

The genetics analysis using fragments of the *cox1* gene, ENM, and dispersal models performed in this study showed that the dominant octopus species in the shallow waters of Western Tropical Atlantic also inhabit the shallow waters of tropical Eastern Atlantic. The Bayesian phylogenetic reconstruction revealed that two octopus samples collected in São Tomé Island belong to a monophyletic and well-supported *O. insularis* clade. In addition, ENM showed that Suriname, São Pedro and São Paulo archipelago, and Western Africa had highly suitable regions (~0.40 of suitability). At the same time, dispersal models pointed out that Suriname, São Pedro and São Paulo archipelago could have been a source of paralarvae to Western Africa.

The long dispersal route from West to East Atlantic could impede the species population settlement on the African islands. However, considering the duration of the species larval period (Roura et al. 2019), high fecundity (Lima et al. 2014a), and the high tolerance of paralarvae to environmental variations (Ángeles-González et al. 2020), the dispersal model demonstrated that *O. insularis* paralarvae could potentially reach Atlantic African seamounts via ocean currents under optimal current conditions after 30-50 days.

Previous studies applying species distribution modeling have pointed out the possibility of *O. insularis* suitable niche in the eastern Atlantic (Lima et al. 2020); nevertheless, this study provides the first evidence of *O. insularis* as a trans-Atlantic species. Updated results of ENM obtained here corroborate the study by Lima et al. (2020) as they show that *O. insularis* can be widely distributed in the Americas and African coast due to its high temperatures (32 °C) and salinities (36-42 PSU) tolerances as observed in the field. Indeed, according to the ENM, the *O. insularis* distribution may be limited mainly by low temperatures and salinities; however, as temperatures increase due to climate change, this species may likely invade higher latitudes (Lima et al. 2020).

The North Equatorial Countercurrent (NECC) influences the connectivity dispersal route towards western Africa. The mean eastward velocity for the NECC is 42 cm s⁻¹, and maximum

20

389 velocities of up 147 cm s^{-1} in the western section of the current (Fratantoni 2001). The

390 hatchlings from São Pedro and São Paulo would arrive at the African coast after 30 (maximum

391 velocity) to 116 days (mean velocity), hypothetically within the larval duration range of the

392 species and in agreement with the dispersal models results. Moreover, the connectivity route

393 coincides with the region of high primary productivity in the Atlantic (Tilstone et al. 2009), which

394 may favor paralarvae survival due to greater food availability. It is important to point out that

395 NECC eastern flow is higher during the boreal summer (June-August) and early fall

396 (September) (Carton and Katz, 1990). Such trends could explain the higher potential

397 connectivity during May-June-July for most years, as paralarvae dispersing thorough NECC

398 could travel eastward faster. The high fecundity of *O. insularis* (68,502 to 120,166) (Lima et

399 al. 2014a) and the small eggs size (~ 2.5 mm) (Lenz et al. 2015) facilitate the paralarvae to be

400 faster carried out by the currents. In addition, the high thermal tolerance of the embryos

401 (Ángeles-González et al. 2020), possibly allows the paralarvae to survive in a wide range of

402 temperatures.

403 Both phylogenetic reconstruction and genetic distance analyses (Tamura-Nei model) pointed

404 out that *O. insularis* from São Tomé Island is part of the Ascension and Saint Helena

405 populations. The African haplotype is also in the same clade of *O. insularis* from Brazil's

406 Northeast coast and oceanic islands. These findings suggest that the African population

407 probably originated from the dispersion of individuals from the Western Atlantic, which agrees

408 with the results of the dispersal model. The haplotype network constructed by Lima et al.

409 (2022) also showed that Saint Helena and Ascension specimens are closely related to

410 individuals from Northeast Brazil. The phylogenetic analysis performed in this study also

411 showed low genetic distances between *O. oculifer* and *O. mimus* (1.06-1.27%), indicating they

412 belong to the same species, which is in agreement with Acosta-Jofré et al. (2012) and Vandez-

413 Cibrián et al. (2020) findings.

414 The planktonic larvae of many other marine species can successfully travel long distances

415 until finding a suitable area for settlement (Cowen and Sponaugle 2009). According to Joyeux

416 et al. (2001), five species of marine fishes have apparently made the eastward transatlantic

417 crossing, two of which are probably recent arrivals, and three established local populations.

418 Lessios et al. (1999) suggest that populations of the sea urchin *Eucidaris tribuloides* (Lamark,

419 1816) from the west coast of Africa and the Caribbean Sea are also connected by recent gene

420 flow. Nunes et al. (2011) assessed connectivity patterns in broadly distributed amphi-Atlantic

421 corals and found species from Brazil and Africa with identical alleles or 1–2 mutations

422 differences.

423 The genetic analyses of these trans-Atlantic taxa aforementioned show low current

424 connectivity between distant populations. The gene flow was probably more frequent in the

425 Pleistocene during the Last Glacial Period (LGP) (110,00-15,000 kya), when the sea level was

426 approximately 120 m lower than today, rising again around 14.5 kya (Lambeck et al. 2014;

427 Ludt & Rocha 2015). Throughout this period, the ocean thermohaline circulation were similar

428 to present days (Yu et al. 1996; Watkins et al. 2007). The shallow ocean depths on continental

429 shelves and seamounts probably favoured transcontinental movement and population

430 expansions. During the trajectory to Western Africa, paralarvae may find seamounts that could

431 be useful as stepping-stones to reach African islands. However, they are currently too deep

432 (bathymetry > 100 m) for settlement to occur. The populations of octopus species with wide

433 distribution are commonly structured over a geographic area (Van Nieuwenhove et al. 2019).

434 Indeed, Lima et al. (2022) demonstrated that populations of *O. insularis* are genetically

435 structured along their distribution range, with low gene flow between both Atlantic coasts.

436 Therefore, considering the current low genetic connectivity between Africa and South America

437 (Lima et al. 2022), we can hypothesize that seamounts in the tropical Atlantic were essential

438 pathways of population connectivity during the LGP.

439 Although our dispersal model was helpful to propose the hypothesis of potential connectivity

440 between South America and Africa, there is a lack of information about the paralarva stage of

441 *O. insularis,* which difficult the addition of biological parameters to the model to increase

442 reliability. For instance, studies have shown that paralarvae vertical diel behaviour can lead to

443 different dispersal patterns, allowing retention or oceanic dispersal of paralarvae (Roura et al.

444 2016, 2019). Particularly, Roura et al. (2019) identified a coastal-oceanic dispersal pattern for

445 *O. vulgaris* (paralarvae were reported between the continental shelf and continental slope),

446 suggesting that the dispersal capacity would be lower for biological entities than for particle

447 simulations (Freire et al. 2021). However, the paralarvae ability to reach seamounts less than

448 100 m depth may have been higher during the Pleistocene, reducing the time necessary for

449 the paralarva to drift.

450 The particles released in Trindade and Martim Vaz archipelago (SW Atlantic) differed greatly

451 from the other zones since the dispersal was almost non-existent, suggesting self-recruitment

452 in this region. These islands are under the influence of the South Atlantic Subtropical Gyre,

453 which originated from the Brazil Current and the South Equatorial Current (Lumpkin and

454 Garzoli 2005; Silveira et al. 2000). The interaction of the Brazil Current with the region's

455 complex topography (Victoria-Trindade seamount) promotes the formation of cyclonic and

456 anticyclonic meanders that can give rise, among others, to the Vitória Vortex (Schmid et al.

457 1995; Campos 2006). The formation of these vortices and closed recirculation cells may be

458 responsible for larval retention in the region, making it difficult for paralarvae to disperse to

459 distant areas (Swearer et al. 1999). Lima et al. (2022) showed that the populations of *O.*

460 *insularis* from Alagoas, Bahia, and Trindade and Martin Vaz are highly structured compared

461 to populations from the other locations of the Northeast Coast of Brazil, probably due to the

462 low potential for dispersion caused by the presence of these eddies. Using genetic data and

463 Lagrangian dispersal models, Freire et al. (2021) also identified the same pattern for the

464 crustacean *Grapsus grapsus* (Linnaeus, 1758) in the Trindade and Martin Vaz islands.

465 The octopus fisheries in some African countries of the eastern Atlantic coast have been under-

466 reported on a massive scale (Sauer et al. 2021), mainly in the Gulf of Guinea countries, where

467 São Tomé and Príncipe islands are located (Area 34 FAO). There are three main stocks of

468 "*Octopus vulgaris*" in the FAO area 34: Dakhla, Cape Blanc, and Senegal-Gambia, reported

469 either as fully exploited or overexploited (Alder and Sumalia 2004). The estimate of the *O.*

470 *vulgaris* total catch in this area is around 60,000 t on average, with a peak of over 330,000 t

471 per year (FAO 2011; Sauer et al. 2021).

472 The new record of *O. insularis* in Africa raises important questions regarding regional fisheries

473 management. The octopus fisheries in São Tomé and Príncipe islands are performed mainly

474 by spearfishing in shallow waters (Maia et al. 2018b). There is little information on the number

475 of octopuses captured through this fishery. Still, according to Porriños (2021), fishers can

476 catch up to 100 to 500 kg of octopuses in a single fishing trip. In addition, the new octopus

477 species indicated in this study may also be part of the target octopus stock in São Tomé Island.

478 There is no specific regulation for octopus fishing in São Tomé and Príncipe, and little is known

479 about the biology and ecology of octopus species in this region. For this reason, it is urgent

480 that further studies on cephalopod diversity, as well as the species composition of the octopus

481 fishery stock, are carried out for the successful management of this important fishery resource.

482 Considering that *O. insularis* is highly tolerant to environmental variations and very adapted to

483 warm shallow waters, there is a possibility that these stocks have a mixed composition (*O.*

484 *vulgaris*, *O. insularis*, and the new species) and therefore, the octopus fisheries must follow

485 management measures suitable for each species.

486

5. Conclusion

488 The genetic results of this study extended the distribution of *O. insularis* to São Tomé and

489 Príncipe islands, confirming that this is the most widely distributed octopus species in the

490 tropical Atlantic. The ENM suggests that the Americas and Western Africa tropical regions are

491 suitable for the species. Finally, the passive dispersal model showed that the *O. insularis*

492 *paralarvae* could potentially cross the Atlantic Ocean and reach the African coast, even though

493 we hypothesized that the current dispersal is occasional and was more common during the

494 lower sea-level glaciation periods in the Miocene–Pliocene.

495 Studies on the biology, ecology, and fishing of octopus in the Gulf of Guinea are scarce.

496 However, correctly identifying the species that compose a fishery stock is crucial for monitoring

497 population fluctuations and preventing species overexploitation (Lima et al. 2017; Tillet et al.

498 2012; Ward 2000). New studies on integrative taxonomy and fishery biology can correctly

499 identify the species that compose these octopus stocks so effective management measures

500 can be applied, ensuring the sustainable exploitation of these species.

501

507

References

509 Acosta-Jofré, M.S., Sahade, R., Laudien, J., Chiappero, M.B., 2012. A contribution to the

510   understanding of phylogenetic relationships among species of the genus *Octopus*

511   (Octopodidae: Cephalopoda). Sci. Mar. 76, 311–318.

512   https://doi.org/10.3989/scimar.03365.03B

513 Aiello-Lammens, M.E., Boria, R.A., Radosavljevic, A., Vilela, B., Anderson, R.P., 2015.

514   spThin: An R package for spatial thinning of species occurrence records for use in

515   ecological niche models. Ecography. 38, 541–545. https://doi.org/10.1111/ecog.01132

516 Alder, J., Sumaila, U.R., 2004. Western Africa: A fish basket of Europe past and present. J.

517   Environ. Dev. 13, 156–178. https://doi.org/10.1177/1070496504266092

518 Allcock, A.L., Strugnell, J.M., Ruggiero, H., Collins, M.A., 2006. Redescription of the deep-

519   sea octopod *Benthoctopus normani* (Massy 1907) and a description of a new species

25

520   from the Northeast Atlantic. Mar. Biol. Res. 2, 372–387.

521   https://doi.org/10.1080/17451000600973315

522 Álvarez-Noriega, M., Burgess, S.C., Byers, J.E., Pringle, J.M., Wares, J.P., Marshall, D.J.,

523   2020. Global biogeography of marine dispersal potential. Nat. Ecol. Evol. 4, 1196–

524   1203. https://doi.org/10.1038/s41559-020-1238-y

525 Amado, E.M., Souza-Bastos, L.R., Vidal, E.A.G., Leite, T.S., Freire, C.A., 2015. Different

526   abilities to regulate tissue hydration upon osmotic challenge in vitro, in the cephalopods

527   *Octopus vulgaris* and *O. insularis.* Mar. Freshw. Behav. Physiol. 48, 205–211.

528   https://doi.org/10.1080/10236244.2015.1024078

529 Amor, M.D., Norman, M.D., Cameron, H.E., Strugnell, J.M., 2014. Allopatric speciation within

530   a cryptic species complex of Australasian octopuses. PLoS One 9, 1–6.

531   https://doi.org/10.1371/journal.pone.0098982

532 Amor, M.D., Laptikhovsky, V., Norman, M.D., Strugnell, J.M., 2017. Genetic evidence

533   extends the known distribution of *Octopus insularis* to the mid-Atlantic islands

534   Ascension and St Helena. J. Mar. Biol. Assoc. United Kingdom 97, 753–758.

535   https://doi.org/https://doi.org/10.1017/S0025315415000958

536 Ángeles-González, L.E., Lima, F.D., Caamal-Monsreal, C., Díaz, F., Rosas, C., 2020.

537   Exploring the effects of warming seas by using the optimal and pejus temperatures of

538   the embryo of three Octopoda species in the Gulf of Mexico. J. Therm. Biol. 94,

539   102753. https://doi.org/10.1016/j.jtherbio.2020.102753

540 Assis, J., Tyberghein, L., Bosch, S., Verbruggen, H., Serrão, E.A., De Clerck, O., 2017. Bio-

541   ORACLE v2.0: Extending marine data layers for bioclimatic modelling. Glob. Ecol.

542   Biogeogr. 27, 277–284. https://doi.org/10.1111/geb.12693

543 Avendaño, O., Roura, Á., Cedillo-Robles, C.E., González, Á.F., Rodríguez-Canul, R.,

544   Velázquez-Abunader, I., Guerra, Á., 2020. *Octopus americanus*: a cryptic species of

545   the O. vulgaris species complex redescribed from the Caribbean. Aquat. Ecol. 54, 909–

546   925. https://doi.org/10.1007/s10452-020-09778-6

547   Barve, N., Barve, V., Jiménez-Valverde, A., Lira-Noriega, A., Maher, S.P., Peterson, A.T.,

548   Soberón, J., Villalobos, F., 2011. The crucial role of the accessible area in ecological

549   niche modeling and species distribution modeling. Ecol. Modell. 222, 1810–1819.

550   https://doi.org/10.1016/j.ecolmodel.2011.02.011

551   Bastos, P., Vieira, G.C., 2018. Maintenance of *Octopus vulgaris* Type II paralarvae in an

552   estuarine area. Rev. Bras. Zootec. 47, 1-7. https://doi.org/10.1590/rbz4720170009

553   Batista, A.T., Leite, T.S., 2016. *Octopus insularis* (Cephalopoda: Octopodidae) on the

554   tropical coast of Brazil: Where it lives and what it eats. Brazilian J. Oceanogr. 64, 353–

555   364. https://doi.org/10.1590/S1679-87592016123406404

556   Batista, B.B., Matthews-Cascon, H., Marinho, R.A., Kikuchi, E., Haimovici, M., 2021. The

557   growth and population dynamics of *Octopus insularis* targeted by a pot longline fishery

558   in north-eastern Brazil. J. Mar. Biol. Assoc. United Kingdom 101, 935–946.

559   https://doi.org/10.1017/S0025315421000898

560   Bouth, H.F., Leite, T.S., de Lima, F.D., Oliveira, J.E.L., 2011. Atol das Rocas: An oasis for

561   *Octopus insularis* juveniles (Cephalopoda: Octopodidae). Zoologia 28, 45–52.

562   https://doi.org/10.1590/S1984-46702011000100007

563   Boyle, P., Rodhouse, P.G., 2005. Cephalopods: ecology and fisheries. Blackwell Science,

564   Oxford.

565   Cabral, H., Drouineau, H., Teles-Machado, A., Pierre, M., Lepage, M., Lobry, J., Reis-

566   Santos, P., Tanner, S.E., 2021. Contrasting impacts of climate change on connectivity

567   and larval recruitment to estuarine nursery areas. Prog. Oceanogr. 196, 102608.

568   https://doi.org/10.1016/j.pocean.2021.102608

569   Campos, E.J.D., 2006. Equatorward translation of the Vitoria Eddy in a numerical simulation.

570   Geophys. Res. Lett. 33, 1–5. https://doi.org/10.1029/2006GL026997

571   Carranza, S., Arnold, E.N., 2003. Investigating the origin of transoceanic distributions:

572   mtDNA shows *Mabuya* lizards (Reptilia, Scincidae) crossed the Atlantic twice. Syst.

573   Biodivers. 1, 275–282. https://doi.org/10.1017/S1477200003001099

574 Carton, J.A., Katz, E.J., 1990. Estimates of the Zonal Slope and Seasonal Transport of the

575 Atlantic North Equatorial Countercurrent. J. Geophys. Res. 95, 3091–3100.

576 https://doi.org/doi.org/10.1029/JC095iC03p03091

577 Chamberlain, S., Barve, V., Mcglinn, D., Oldoni, D., Desmet, P., Geffert, L., Ram, K., 2022.

578 rgbif: Interface to the Global Biodiversity Information Facility API_. R package version

579 3.6.0.

580 Cowen, R.K., Sponaugle, S., 2009. Larval dispersal and marine population connectivity.

581 Ann. Rev. Mar. Sci. 1, 443–466.

582 https://doi.org/10.1146/annurev.marine.010908.163757

583 Drummond, A.J., Suchard, M.A., Xie, D., Rambaut, A., 2012. Bayesian phylogenetics with

584 BEAUti and the BEAST 1.7. Mol. Biol. Evol. 29, 1969–1973.

585 https://doi.org/10.1093/molbev/mss075

586 Elith, J., Kearney, M., Phillips, S., 2010. The art of modelling range-shifting species. Methods

587 Ecol. Evol., 1, 330–342. https://doi.org/10.1111/j.2041-210X.2010.00036.x

588 FAO, 2011. Review of the state of world marine fishery resources. FAO Fish. Aquac. Tech.

589 Pap. 569. FAO, Rome.

590 Flores-Valle, A., Pliego-Cárdenas, R., Jiménez-Badillo, L., Arredondo-Figueroa, J.L.,

591 Barriga-Sosa, I.D.L.A., 2018. First Record of *Octopus insularis* Leite and Haimovici,

592 2008 in the Octopus Fishery of a Marine Protected Area in the Gulf of Mexico. J.

593 Shellfish Res. 37, 221–227. https://doi.org/10.2983/035.037.0120

594 Folmer, O., Black, M., Hoeh, W., Lutz, R., Vrijenhoek, R., 1994. DNA primers for

595 amplification of mitochondrial Cytochrome c Oxidase Subunit I from diverse metazoan

596 invertebrates. Mol. Mar. Biol. Biotechnol. 3, 294–299.

597 Fratantoni, D.M., 2001. North Atlantic Surface Circulation during the 1990's Observed with

598 Satellite-Tracked Drifters. J. Geophys. Res. 22, 22067–22093.

599 Freire, A.S., Teschima, M.M., Brandão, M.C., Iwasa-Arai, T., Sobral, F.C., Sasaki, D.K.,

600 Agostinis, A.O., Pie, M.R., 2021. Does the transport of larvae throughout the south

601 Atlantic support the genetic and morphometric diversity of the Sally Lightfoot Crabs

602   *Grapsus grapsus* (Linnaeus, 1758) and *Grapsus adscensionis* (Osbeck, 1765)

603   (Decapoda: Grapsidae) among the oceanic islands. J. Mar. Syst. 223.

604   https://doi.org/10.1016/j.jmarsys.2021.103614

605   Gaither, M.R., Bernal, M.A., Coleman, R.R., Bowen, B.W., Jones, S.A., Simison, W.B.,

606   Rocha, L.A., 2015. Genomic signatures of geographic isolation and natural selection in

607   coral reef fishes. Mol. Ecol. 24, 1543–1557. https://doi.org/10.1111/mec.13129

608   Gray, L.A., Bisonó León, A.G., Rojas, F.E., Veroneau, S.S., Slocum, A.H., 2021. Caribbean-

609   Wide, Negative Emissions Solution to Sargassum spp. Low-Cost Collection Device and

610   Sustainable Disposal Method. Phycology 1, 49–75.

611   https://doi.org/10.3390/phycology1010004

612   González-Gómez, R., Meiners-Mandujano, C., Morillo-Velarde, P.S., Jiménez-Badillo, L.,

613   Markaida, U., 2020. Reproductive Dynamics and Population Structure of *Octopus*

614   *insularis* From the Veracruz Reef System Marine Protected Area, Mexico. Fish. Res.

615   221, 105385. https://doi.org/10.1016/j.fishres.2019.105385

616   Hedgecock, D., 1986. Is Gene Flow From Pelagic Larval Dispersal Important in the

617   Adaptation and Evolution of Marine Invertebrates? Bull. Mar. Sci. 39, 550–564.

618   Hellberg, M.E., 2009. Gene Flow and Isolation among Populations of Marine Animals. Annu.

619   Rev. Ecol. Evol. Syst. 40, 291–310.

620   https://doi.org/10.1146/annurev.ecolsys.110308.120223

621   Houle, A., 1998. Floating Islands: A Mode of Long-Distance Dispersal for Small and

622   Medium- Sized Terrestrial Vertebrates. Divers. Distrib, 4, 201–216.

623   Jordan, C., Cusack, C., Tomlinson, M.C., Meredith, A., McGeady, R., Salas, R., Gregory, C.,

624   Croot, P.L., 2021. Using the Red Band Difference Algorithm to Detect and Monitor a

625   Karenia spp. Bloom Off the South Coast of Ireland, June 2019. Front. Mar. Sci. 8.

626   https://doi.org/10.3389/fmars.2021.638889

627   Joyeux, J., Floeter, S.R., Ferreira, C.E.L., Gasparini, J.L., 2001. Biogeography of tropical

628   reef fishes: the South Atlantic puzzle. J. Biogeogr. 28, 831–841.

629   https://doi.org/10.1046/j.1365-2699.2001.00602.x

29

630 Juárez, O., Rosas, C., Arenta-Ortiz, M., 2012. Phylogenetic relationships *of Octopus maya*

631   revealed by mtDNA sequences. Ciencias Mar. 38, 563–575.

632   https://doi.org/10.7773/cm.v38i3.1962

633 Kaneko, N., Kubodera, T., Iguchis, A., 2011. Taxonomic study of shallow-water octopuses

634   (Cephalopoda: Octopodidae) in Japan and adjacent waters using mitochondrial genes

635   with perspectives on octopus DNA barcoding. Malacologia 54, 97–108.

636   https://doi.org/10.4002/040.054.0102

637 Kass, J.M., Muscarella, R., Galante, P.J., Bohl, C.L., Pinilla-Buitrago, G.E., Boria, R.A.,

638   Soley-Guardia, M., Anderson, R.P., 2021. ENMeval 2.0: Redesigned for customizable

639   and reproducible modeling of species' niches and distributions. Methods Ecol. Evol. 12,

640   1602–1608. https://doi.org/10.1111/2041-210X.13628

641 Kearse, M., Moir, R., Wilson, A., Stones-Havas, S., Cheung, M., Sturrock, S., Buxton, S.,

642   Cooper, A., Markowitz, S., Duran, C., Thierer, T., Ashton, B., Meintjes, P., Drummond,

643   A., 2012. Geneious Basic: An integrated and extendable desktop software platform for

644   the organization and analysis of sequence data. Bioinformatics 28, 1647–1649.

645   https://doi.org/10.1093/bioinformatics/bts199

646 Lalire, M., Gaspar, P., 2019. Modeling the active dispersal of juvenile leatherback turtles in

647   the North Atlantic Ocean. Mov. Ecol. 7, 1–18. https://doi.org/doi.org/10.1186/s40462-

648   019-0149-5

649 Lambeck, K., Rouby, H., Purcell, A., Sun, Y., Sambridge, M., 2014. Sea level and global ice

650   volumes from the Last Glacial Maximum to the Holocene. PNAS 111, 15296–15303.

651   https://doi.org/10.1073/pnas.1411762111

652 Lapègue, S., Boutet, I., Leitão, A., Heurtebise, S., Garcia, P., Thiriot-Quiévreux, C., Boudry,

653   P., 2002. Trans-Atlantic Distribution of a Mangrove Oyster Species Revealed by 16S

654   mtDNA and Karyological Analyses. Biol. Bull. 202, 232–242.

655   https://doi.org/10.2307/1543473

656 Leite, T.S., Haimovici, M., Molina, W., Warnke, K., 2008. Morphological and genetic

657   description of *Octopus insularis*, a new cryptic species in the *Octopus vulgaris* complex

658   (Cephalopoda: Octopodidae) from the tropical southwestern Atlantic. J. Molluscan Stud.

659   74, 63–74. https://doi.org/10.1093/mollus/eym050

660   Leite, T.S., Haimovici, M., Mather, J., Oliveira, J.E.L., 2009. Habitat, distribution, and

661   abundance of the commercial octopus (*Octopus insularis*) in a tropical oceanic island,

662   Brazil: information for management of an artisanal fishery inside a marine protected

663   area. Fish. Res. 98, 85–91. https://doi.org/10.1016/j.fishres.2009.04.001

664   Leite, T.S., Batista, A.T., Lima, F.D., Barbosa, J.C., Mather, J., 2016. Geographic variability

665   of *Octopus insularis* diet: From oceanic island to continental populations. Aquat. Biol.

666   25, 17–27. https://doi.org/10.3354/ab00655

667   Lellouche, J.-M., Bourdallé-Badie, R., Greiner, E., Garric, G., Melet, A., Bricaud, C.,

668   Legalloudec, O., Hamon, M., Candela, T., Regnier, C., Drevillon, M., 2021a. The

669   Copernicus global 1/12° oceanic and sea ice reanalysis.

670   https://doi.org/10.5194/egusphere-egu21-14961, 2021

671   Lellouche, J.M., Greiner, E., Bourdallé-Badie, R., Garric, G., Melet, A., Drévillon, M.,

672   Bricaud, C., Hamon, M., Le Galloudec, O., Regnier, C., Candela, T., Testut, C.-E.,

673   Gasparin, F., Ruggiero, G., Benkiran, M., Drillet, Y., Pierre-Yves, L.T., 2021b. The

674   Copernicus Global 1/12° Oceanic and Sea Ice GLORYS12 Reanalysis. Front. Earth

675   Sci. 9, 1–27. https://doi.org/10.3389/feart.2021.698876

676   Lenz, T.M., Elias, N.H., Leite, T.S., Vidal, E.A.G., 2015. First description of the eggs and

677   paralarvae of the tropical octopus, *Octopus insularis*, under culture conditions. Am.

678   Malacol. Bull. 33, 101–109. https://doi.org/10.4003/006.033.0115

679   Lessios, H.A., Kessing, B.D., Robertson, D.R., Paulay, G., 1999. Phylogeography of the

680   pantropical sea urchin *Eucidaris* in relation to land barriers and ocean currents.

681   Evolution (N. Y). 53, 806–817. https://doi.org/10.1111/j.1558-5646.1999.tb05374.x

682   Lett, C., Verley, P., Mullon, C., Parada, C., Brochier, T., Penven, P., Blanke, B., 2008. A

683   Lagrangian tool for modelling ichthyoplankton dynamics. Environ. Model. Softw. 23,

684   1210–1214. https://doi.org/10.1016/j.envsoft.2008.02.005

685   Librado, P., Rozas, J.,2009. DnaSP v5: a software for comprehensive analysis of DNA

686   polymorphism data. Bioinformatics 25:1451–1452. https://doi.org/10.1093/bioinforma

687   tics/ btp187

688   Lima, F.D., Leite, T.S., Haimovici, M., Lins Oliveira, J.E., 2014a. Gonadal development and

689   reproductive strategies of the tropical octopus (*Octopus insularis*) in northeast Brazil.

690   Hydrobiologia 725, 7–21. https://doi.org/10.1007/s10750-013-1718-z

691   Lima, F., Leite, T., Haimovici, M., Nobrega, M., Lins Oliveira, J., 2014b. Population structure

692   and reproductive dynamics of *Octopus insularis* (Cephalopoda: Octopodidae) in a

693   coastal reef environment along northeastern Brazil. Fish. Res. 152, 86–92.

694   https://doi.org/10.1016/j.fishres.2013.08.009

695   Lima, F.D., Berbel-Filho, W.M., Leite, T.S., Rosas, C., Lima, S.M.Q., 2017. Occurrence of

696   *Octopus insularis* Leite and Haimovici, 2008 in the Tropical Northwestern Atlantic and

697   implications of species misidentification to octopus fisheries management. Mar.

698   Biodivers. 47, 723–734. https://doi.org/10.1007/s12526-017-0638-y

699   Lima, F., Ángeles-González, L., Leite, T., Lima, S., 2020. Global climate changes over time

700   shape the environmental niche distribution of *Octopus insularis* in the Atlantic Ocean.

701   Mar. Ecol. Prog. Ser. 652, 111–121. https://doi.org/10.3354/meps13486

702   Lima, L.S., Gherardi, D.F.M., Pezzi, L.P., Passos, L.G. dos, Endo, C.A.K.,

703   Quimbayo, J.P., 2021. Potential changes in the connectivity of marine protected

704   areas driven by extreme ocean warming. Sci. Rep. 11, 1–12.

705   https://doi.org/10.1038/s41598-021-89192-6

706   Lima, F.D., Leite, T.S., Lima, S.M.Q., 2022. Seamounts and oceanic currents drive the

707   population structure of *Octopus insularis* in the Southwest Tropical Atlantic. Aquat.

708   Ecol. https://doi.org/10.1007/s10452-022-09955-9

709   Ludt, W.B., Rocha, L.A., 2015. Shifting seas: The impacts of Pleistocene sea-level

710   fluctuations on the evolution of tropical marine taxa. J. Biogeogr. 42, 25–38.

711   https://doi.org/10.1111/jbi.12416

712 Lumpkin, R., Garzoli, S.L., 2005. Near-surface circulation in the Tropical Atlantic Ocean.

713   Deep. Res. Part I 52, 495–518. https://doi.org/10.1016/j.dsr.2004.09.001

714 Macías, D., Prieto, L., García-Gorriz, E., 2021. A model-based management tool to predict

715   the spread of Physalia physalis in the Mediterranean Sea. Minimizing risks for coastal

716   activities. Ocean Coast. Manag. 212, 105810.

717   https://doi.org/10.1016/j.ocecoaman.2021.105810

718 Maia, H.A., Morais, R.A., Quimbayo, J.P., Dias, M.S., Sampaio, C.L.S., Horta, P.A., Ferreira,

719   C.E.L., Floeter, S.R., 2018a. Spatial patterns and drivers of fish and benthic reef

720   communities at São Tomé Island, Tropical Eastern Atlantic. Mar. Ecol. 39.

721   https://doi.org/10.1111/maec.12520

722 Maia, H.A., Morais, R.A., Siqueira, A.C., Hanazaki, N., Floeter, S.R., Bender, M.G., 2018b.

723   Shifting baselines among traditional fishers in São Tomé and Príncipe islands, Gulf of

724   Guinea. Ocean Coast. Manag. 154, 133–142.

725   https://doi.org/10.1016/j.ocecoaman.2018.01.006

726 Melis, R., Vacca, L., Cuccu, D., Mereu, M., Cau, A., Follesa, M.C., Cannas, R., 2018.

727   Genetic population structure and phylogeny of the common octopus *Octopus vulgaris*

728   Cuvier, 1797 in the western Mediterranean Sea through nuclear and mitochondrial

729   markers. Hydrobiologia 807, 277–296. https://doi.org/10.1007/s10750-017-3399-5

730 Muscarella, R., Galante, P.J., Soley-Guardia, M., Boria, R.A., Kass, J.M., Uriarte, M.,

731   Anderson, R.P., 2014. ENMeval: An R package for conducting spatially independent

732   evaluations and estimating optimal model complexity for <scp>Maxent</scp> ecological

733   niche models. Methods Ecol. Evol. 5, 1198–1205. https://doi.org/10.1111/2041-

734   210X.12261

735 Nunes, F.L.D., Norris, R.D., Knowlton, N., 2011. Long distance dispersal and connectivity in

736   Amphi-Atlantic corals at regional and basin scales. PLoS One 6.

737   https://doi.org/10.1371/journal.pone.0022298

738 O'brien, C.E., Bennice, C.O., Leite, T., 2021. A field guide to distinguishing *Octopus insularis*

739   and *Octopus americanus* (Octopoda: Octopodidae). Zootaxa 5060, 589–594.

33

740   https://doi.org/10.11646/zootaxa.5060.4.8

741 Peliz A, Dubert J., Marchesiello P., Teles-Machado A., (2007) Surface circulation in the Gulf

742   of Cadiz: Model and mean flow structure. J Geophys Res Ocean 112:1–20.

743   https://doi.org/10.1029/2007JC004159

744 Peterson, R.G., Stramma, L., 1991. Upper-level circulation in the South Atlantic Ocean.

745   Prog. Oceanogr. 26, 1–73. https://doi.org/10.1016/0079-6611(91)90006-8

746 Pliego-Cárdenas, R., Hochberg, F.G., León, F.J.G. De, Barriga-Sosa, I.D.L.A., 2014. Close

747   genetic relationships between two American cctopuses: *Octopus hubbsorum* Berry,

748   1953, and *Octopus mimus* Gould, 1852. J. Shellfish Res. 33, 293–303.

749   https://doi.org/10.2983/035.033.0128

750 Posada, D., 2008. jModelTest: Phylogenetic model averaging. Mol. Biol. Evol. 25, 1253–

751   1256. https://doi.org/10.1093/molbev/msn083

752 Porriños, G., da Rocha, N., da Graça, M., Santos, A., Nazaré, L., Espírito-Santo, S.,

753   Madruga, L., 2021. Characterisation of artisanal fisheries in São Tomé and Príncipe

754   through participatory, smartphone-based landing surveys, Report for Fauna and Flora

755   International.

756 Provoost, P., Bosch, S., 2022. robis: Ocean Biodiversity Information System (OBIS) Client. R

757   package version 2.10.1.

758 Quinteiro, J., Rodríguez-Castro, J., Rey-Méndez, M., Henríquez, N.G., 2020.

759   Phylogeography of the insular populations of common octopus, *Octopus vulgaris*

760   cuvier, 1797, in the atlantic macaronesia. PLoS One 15, 1–19.

761   https://doi.org/10.1371/journal.pone.0230294

762 Ramos, J.E., Pecl, G.T., Moltschaniwskyj, N.A., Semmens, J.M., Souza, C.A., Strugnell,

763   J.M., 2018. Population genetic signatures of a climate change driven marine range

764   extension. Sci. Rep. 8, 9558. https://doi.org/10.1038/s41598-018-27351-y

765 R Core Team, 2022. R: A Language and Environment for Statistical Computing.

766 Radosavljevic, A., Anderson, R.P., 2014. Making better Maxent models of species

767   distributions: Complexity, overfitting and evaluation. J. Biogeogr. 41, 629–643.

768   https://doi.org/10.1111/jbi.12227

769 Rambaut, A., Suchard, M.A., Xie, D., Drummond, A.J., 2014. Tracer v1.6.0. Available at

770   http://tree.bio.ed.ac.uk/software/tracer/.

771 Renner, S., 2004. Plant dispersal across the tropical Atlantic by wind and sea currents. Int. J.

772   Plant Sci. 165. https://doi.org/10.1086/383334

773 Ritschard, E.A., Guerrero-Kommritz, J., Sanchez, J.A., 2019. First molecular approach to the

774   octopus fauna from the southern Caribbean. PeerJ 2019, 1–14.

775   https://doi.org/10.7717/peerj.7300

776 Rocha, L.A., Rocha, C.R., Robertson, D.R., Bowen, B.W., 2008. Comparative

777   phylogeography of Atlantic reef fishes indicates both origin and accumulation of

778   diversity in the Caribbean. BMC Evol. Biol. 8, 1–16. https://doi.org/10.1186/1471-2148-

779   8-157

780 Roura, Á., Antón Álvarez-Salgado, X., González, Á.F., Gregori, M., Rosón, G., Otero, J.,

781   Guerra, Á., 2016. Life strategies of cephalopod paralarvae in a coastal upwelling

782   system (NW Iberian Peninsula): Insights from zooplankton community and spatio-

783   temporal analyses. Fish. Oceanogr. 25, 241–258. https://doi.org/10.1111/fog.12151

784 Roura, Á., Amor, M., González, Á.F., Guerra, Á., Barton, E.D., Strugnell, J.M., 2019.

785   Oceanographic processes shape genetic signatures of planktonic cephalopod

786   paralarvae in two upwelling regions. Prog. Oceanogr. 170, 11–27.

787   https://doi.org/10.1016/j.pocean.2018.10.005

788 Rudorff, C.A.. G., Lorenzzetti, J.A., Gherardi, D.F.M., Lins-Oliveira, J.E., 2009. Modeling

789   spiny lobster larval dispersion in the Tropical Atlantic. Fish. Res. 96, 206–215.

790   https://doi.org/10.1016/j.fishres.2008.11.005

791 Santana-Cisneros, M.L., Ardisson, P.L., González, Á.F., Mariño-Tapia, I., Cahuich-López,

792   M., Ángeles-González, L.E., Ordoñez-López, U., Velázquez-Abunader, I., 2021.

793   Dispersal modeling of octopoda paralarvae in the Gulf of Mexico. Fish. Oceanogr. 1–

794   14. https://doi.org/10.1111/fog.12555

795 Sauer, W.H.H., Gleadall, I.G., Downey-Breedt, N., Doubleday, Z., Gillespie, G., Haimovici,

796   M., Ibáñez, C.M., Katugin, O.N., Leporati, S., Lipinski, M.R., Markaida, U., Ramos, J.E.,

797   Rosa, R., Villanueva, R., Arguelles, J., Briceño, F.A., Carrasco, S.A., Che, L.J., et al.,

798   2021. World Octopus Fisheries. Rev. Fish. Sci. Aquac. 29, 279–429.

799   https://doi.org/10.1080/23308249.2019.1680603

800 Sbrocco, E.J., Barber, P.H., 2013. MARSPEC: Ocean climate layers for marine spatial

801   ecology. Ecology 94, 979. https://doi.org/10.1890/12-1358.1

802 Sillero, N., Barbosa, A.M., 2021. Common mistakes in ecological niche models. Int. J.

803   Geogr. Inf. Sci. 35, 213–226. https://doi.org/10.1080/13658816.2020.1798968

804 Silveira, I.C.A., Schmidt, A.C.K., Campos, E.J.D., Godoi, S.S., Ikeda, Y., 2000. A Corrente

805   do Brasil ao Largo da Costa Leste Brasileira. Rev. bras. Ocean. 48, 171–183.

806   https://doi.org/10.1136/bmj.j3567

807 Schmid, C., Schäfer, H., Zenk, W., Podestá, G., 1995. The Vitória eddy and its relation to the

808   Brazil Current. J. Phys. Oceanogr. 25, 2532–2546.

809   https://doi.org/https://doi.org/10.1175/1520-0485(1995)025<2532:TVEAIR>2.0.CO;2

810 Spalding, M.D., Fox, H.E., Allen, G.R., Davidson, N., Ferdaña, Z.A., Finlayson, M., Halpern,

811   B.S., Jorge, M.A., Lombana, A.., Lourie, S.A., Martin, K.D., McManus, E., Molnar, J.,

812   Recchia, C., Robertson, J., 2007. Marine Ecoregions of the World: A Bioregionalization

813   of Coastal and Shelf Areas. Bioscience 57, 573–583. https://doi.org/10.1641/B570707

814 Swearer, S.E., Caselle, J.E., Lea, D.W., Warner, R.R., 1999. Larval retention and

815   recruitment in an island population of a coral-reef fish. Nature 402, 799–802.

816   https://doi.org/10.1038/45533

817 Tamura, K., Stecher, G., Peterson, D., Filipski, A., Kumar, S., 2013. MEGA6: Molecular

818   evolutionary genetics analysis version 6.0. Mol. Biol. Evol. 30, 2725–2729.

819   https://doi.org/10.1093/molbev/mst197

820 Teske, P.R., Oosthuizen, A., Papadopoulos, I., Barker, N.P., 2007. Phylogeographic

821   structure of *Octopus vulgaris* in South Africa revisited: Identification of a second lineage

36

822   near Durban harbour. Mar. Biol. 151, 2119–2122. https://doi.org/10.1007/s00227-007-

823   0644-x

824   Tillett, B.J., Field, I.C., Bradshaw, C.J.A., Johnson, G., Buckworth, R.C., Meekan, M.G.,

825   Ovenden, J.R., 2012. Accuracy of species identification by fisheries observers in a

826   north Australian shark fishery. Fish. Res. 127–128, 109–115.

827   https://doi.org/10.1016/j.fishres.2012.04.007

828   Tilstone, G., Smyth, T., Poulton, A., Hutson, R., 2009. Measured and remotely sensed

829   estimates of primary production in the Atlantic Ocean from 1998 to 2005. Deep. Res.

830   Part II Top. Stud. Oceanogr. 56, 918–930. https://doi.org/10.1016/j.dsr2.2008.10.034

831   Valdez-Cibrián, A., Díaz-Santana-iturrios, M., Landa-Jaime, V., Michel-Morfín, J.E., 2020.

832   First detection of an ocellate octopus in the revillagigedos ecoregion, a biodiversity

833   hotspot located in the tropical east Pacific Province. Zookeys 2020, 81–100.

834   https://doi.org/10.3897/zookeys.986.53250

835   Van Nieuwenhove, A.H.M., Ratsimbazafy, H.A., Kochzius, M., 2019. Cryptic diversity and

836   limited connectivity in octopuses: Recommendations for fisheries management. PLoS

837   One 14, 1–20. https://doi.org/10.1371/journal.pone.0214748

838   Villanueva, R., Nozais, C., Boletzky, S. V., 1997. Swimming behaviour and food searching in

839   planktonic *Octopus vulgaris* Cuvier from hatching to settlement. J. Exp. Mar. Bio. Ecol.

840   208, 169–184. https://doi.org/10.1016/S0022-0981(96)026706

841   Villanueva, R., Norman, M.D., 2008. Biology of the planktonic stages of benthic octopuses.

842   Oceanogr. Mar. Biol. An Annu. Rev. 46, 105–202.

843   Ward, R.D., 2000. Genetics in fisheries management. Hydrobiologia 420, 191–201.

844   https://doi.org/10.1023/A:1003928327503

845   Watkins, S.J., Maher, B.A., Bigg, G.R., 2007. Ocean circulation at the Last Glacial

846   Maximum: A combined modeling and magnetic proxy-based study. Paleoceanography

847   22, 1–20. https://doi.org/10.1029/2006PA001281

848 Ylitalo, H. a., Watling, L., Toonen, R.J., 2014. First description of hatchlings and eggs of

849   *Octopus oliveri* (Berry, 1914) (Cephalopoda: Octopodidae). Molluscan Res. 34, 79–83.

850   https://doi.org/10.1080/13235818.2013.860871

851 Yu, E.F., Francois, R., Bacon, M.P., 1996. Similar rates of modern and last-glacial ocean

852   thermohaline circulation inferred from radiochemical data. Nature.

853   https://doi.org/10.1038/379689a0

854 **SUPPLEMENTARY MATERIAL**

855

856 **Molecular data, ecological niche, and dispersal models reveal a Trans-Atlantic**

857 **shallow-water octopus species**

858 Françoise D. Lima, Luís Enrique Ángeles-González, Hugulay Maia, Tatiana S. Leite, Miguel

859 Cahuich-López, Ismael Mariño-Tapia, Mariana L. Santana-Cisneros, Pedro-Luis Ardisson,

860 Sergio M. Q. Lima

861

862 **Table S1.**

863 Sequences of *cox1* gene of octopods species retrieved from GenBank and this study used in
864 the phylogenetic analyses.

865

Species	Local	Accession number	Haplotype	Reference
Octopus americanus	Mexico	MT022413	1	Avendaño et al. 2020
Octopus americanus	United States - Virginia	MH087637	2	Aguilar et al. 2018 (*Unpublished*)
Octopus vulgaris	Azores	MN705281	3	Quinteiro et al. 2020
Octopus vulgaris	Italy	KT008577	4	Melis et al. 2018
Octopus vulgaris	Italy	KT008578	5	Melis et al. 2018
Octopus vulgaris	France	EF016328	6	Allcock et al. 2006
Octopus vulgaris	Canaries	MN705287	7	Quinteiro et al. 2020
Octopus vulgaris	South Africa	DQ683213	7	Teske et al. 2007
Octopus vulgaris	South Africa	DQ683212	7	Teske et al. 2007
Octopus vulgaris	Canaries	MN705309	8	Quinteiro et al. 2020
Octopus vulgaris	Cabo verde	MN705290	9	Quinteiro et al. 2020
Octopus sinensis	Japan	AB430548	10	Kaneko et al. 2011
Octopus tetricus	New Zealand	KJ605259	11	Amor et al. 2014
Octopus tetricus	Autralia - Tasmania	MH289820	12	Ramos et al. 2018
Octopus sp	São Tomé Island	OQ361634	13	present study
Octopus oliveri	Hawaii - USA	KC848885	14	Ylitalo et al. 2014

Octopus briareus	Colombia	MG778069	15	Ritschard et al. 2019
Octopus oculifer	Revillagigedos, Mexico	MN259102	16	Valdez-Cibrián et al. 2020
Octopus oculifer	Revillagigedos, Mexico	MN259101	17	Valdez-Cibrián et al. 2020
Octopus mimus	Chile	GU355924	18	Acosta-Jofré et al. 2012
Octopus taganga	Colombia	MG778063	19	Ritschard et al. 2019
Octopus hummelincki	Brazil	MN933640	20	Lima et al. 2020
Octopus maya	Mexico	KY492363	21	Flores-Valle et al. 2018
Octopus maya	Mexico	GU362545	22	Juarez et al. 2012
Octopus insularis	São Tomé Island	OQ361632	23	present study
Octopus insularis	São Tomé Island	OQ361633	23	present study
Octopus insularis	Ascension and St Helena	KP056552	23	Amor et al. 2017
Octopus insularis	Ascension and St Helena	KP056553	23	Amor et al. 2017
Octopus insularis	Ascension and St Helena	KP056554	23	Amor et al. 2017
Octopus insularis	Ascension and St Helena	KP056555	23	Amor et al. 2017
Octopus insularis	Veracruz/Mexico	MH550422	24	González-Gomez et al. 2018
Octopus insularis	Veracruz/Mexico	MH550423	24	González-Gomez et al. 2018
Octopus insularis	Veracruz/Mexico	MH550424	24	González-Gomez et al. 2018
Octopus insularis	Ceará - Brazil	OM307333	24	Lima et al. 2022
Octopus insularis	Rio Grande do Norte - Brazil	OM307355	25	Lima et al. 2022
Octopus insularis	São Pedro and São Paulo - Brazil	OM307298	26	Lima et al. 2022
Octopus insularis	Trindade island - Brazil	OM307377	27	Lima et al. 2022
Octopus insularis	Bahia - Brazil	OM307312	28	Lima et al. 2022
Octopus bimaculatus	Mexico - Sonora	KT335828	30	Pliego-Cárdenas et al. 2014
Octopus bimaculoides	Mexico	MN180721	31	Pliego-Cárdenas et al. 2020

866

867

868

869

870

871

872

873

874

875

876

877

878

879

880

881

882

883

884

885

886

Figure S1. Binary map of *O. insularis* niche suitability obtained from the suitability map.

Figure S2. Response curves of the environmental and physical variables.

920

921

922 Figure S3. Extrapolation risk map. Positive values indicate no extrapolation risk while red
923 ones indicate risk.

924

925

926 **Supplementary 4:**

927

928 Gifs animation of bimonthly dispersal simulations for the years 2006 to 2015:

929 https://doi.org/10.5281/zenodo.7596276

Figure1

Figure2

1
2
3
4
5
6
7
8
9
10
11
12
13
14
15
16
17
18
19
20
21
22
23
24
25
26
27
28
29
30
31
32
33
34
35
36
37
38
39
40
41
42
43
44
45
46
47
48
49

Figure3

Figure4